7-1995

Binary Star Orbits from Speckle Interferometry. VI. The Nearby Solar-Type Speckle-Spectroscopic Binary HR 6697

Harold McAlister
Georgia State University

William I. Hartkopf
Georgia State University

Brian D. Mason
Georgia State University

Francis C. Fekel
Tennessee State University

Philip A. Ianna
University of Virginia

See next page for additional authors

Recommended Citation

McAlister, H.A.; Hartkopf, W.I.; Mason, B.D.; Fekel, F.C.; Ianna, P.A.; Tokovinin, A.A.; Griffin, R.F.; Culver, R.B. "Binary Star Orbits from Speckle Interferometry. VI. The Nearby Solar-Type Speckle-Spectroscopic Binary HR 6697" Astronomical Journal v.110, p.366 (1995)

BINARY STAR ORBITS FROM SPECKLE INTERFEROMETRY. VI. THE NEARBY SOLAR-TYPE SPECKLE-SPECTROSCOPIC BINARY HR 6697

Harold A. McAlister,[1,2] William I. Hartkopf,[1] and Brian D. Mason[1]
Center for High Angular Resolution Astronomy, Georgia State University, Atlanta, Georgia 30303
Electronic mail: hal@chara.gsu.edu, hartkopf@chara.gsu.edu, mason@chara.gsu.edu

Francis C. Fekel[1,3]
Marshall Space Flight Center, Space Science Laboratory, ES-82, Huntsville, Alabama 35812, and Center of Excellence in Information Systems, Tennessee State University, 330 Tenth Avenue North, Nashville, Tennessee 37203-3401
Electronic mail: fekel@coe.tnstate.edu

Philip A. Ianna[1]
Leander J. McCormick Observatory, The University of Virginia, Charlottesville, Virginia 22903-0818
Electronic mail: pai@fermi.clas.virginia.edu

Andrei A. Tokovinin
Sternberg Astronomical Institute, 119899 University Prospect, 13 Moscow, Russia
Electronic mail: toko@sai.msk.su

R. F. Griffin
The Observatories, Madingley Road, Cambridge, CB3 0HA, United Kingdom
Electronic mail: rfg1@phx.cam.ac.uk

Roger B. Culver[1]
Department of Physics, Colorado State University, Fort Collins, Colorado 80523

Received 1994 December 20; revised 1995 March 6

ABSTRACT

Interferometric, spectroscopic, astrometric, and photometric observations are presented for the nearby solar-type binary HR 6697. The system consists of a G0-2 V primary and a K2-5 V secondary. From a combined solution of the speckle and spectroscopic data the orbital period is 881 days or 2.41 yr, the semimajor axis is 2.1 A.U., the eccentricity is 0.42, and the inclination is 68°. The masses and luminosities are $1.16\pm0.12\ \mathscr{M}_\odot$, $0.77\pm0.05\ \mathscr{M}_\odot$, $1.61\pm0.15\ L_\odot$, and $0.17\pm0.05 L_\odot$. Two independent determinations of the parallax, a trigonometric parallax of $0\farcs0379\pm0\farcs0030$, and an orbital parallax of $0\farcs0375\pm0\farcs0014$, are in excellent agreement and give a mean distance of 26.6 ± 0.9 pc. The system appears to be metal rich relative to the Sun, and space motions do not identify it with any moving group.

1. INTRODUCTION

McAlister & Ianna (1974) first aroused interest in HR 6697=HD 163840=McA 50 [$\alpha=17^h57^m14\fs32$, $\delta=23°59'45\farcs2$ (2000), G2 V, V=6.31] by suggesting that it is a G dwarf in the local solar neighborhood. Preliminary results for its parallax (Culver *et al.* 1981) confirmed this initial supposition, which was based on the MK classification of G2 V by Harlan & Taylor (1970). The published radial velocity data for HR 6697 (Young 1945) suggested that the star might be a long-period spectroscopic binary. Using speckle interferometry, McAlister (1978) resolved the visual components of HR 6697 for the first time in 1976. Halliwell (1981) noted it as a promising candidate for an orbital parallax determination. The continued astrometric observations, as well as its inclusion on the speckle and spectroscopic observing programs of a number of independent observers led to the present collaboration and the analysis of the data presented here.

The significant magnitude difference of the components ($\Delta m_v\sim2.8$ mag) makes the detection of the secondary difficult for both speckle and spectroscopic observers. Nevertheless, we have successfully observed the secondary with both techniques on a number of occasions. The combination of speckle and spectroscopic observations in such circumstances results in the determination of an orbital parallax as well as the individual masses and luminosities of the components, contributing to the database of fundamental stellar properties for nearby stars.

[1]Visiting Astronomer, Kitt Peak National Observatory, National Optical Astronomy Observatories, operated by the Association of Universities for Research in Astronomy, Inc., under contract with the National Science Foundation.
[2]Visiting Astronomer, Canada–France–Hawaii Telescope, operated by the National Research Council of Canada, the Centre National de la Recherche Scientifique de France, and the University of Hawaii.
[3]NRC Senior Research Associate.

 0004-6256/95/110(1)/366/10/$0.90

2. OBSERVATIONS

2.1 Speckle Interferometry

Because of its variable radial velocity and the likelihood that it is a nearby star, HR 6697 was first observed by speckle interferometry in April 1976 and found to be a moderately close system (McAlister 1978). The newly resolved binary (designated as McA 50) was observed at every subsequent opportunity with the Kitt Peak photographic speckle camera at the KPNO 2.1 m and 4 m reflectors between 1976 and 1981 and the GSU ICCD speckle camera at the KPNO 4 m and CFH 3.6 m telescopes. HR 6697 has been observed by the CHARA speckle group on a total of 42 nights between 1976.3 and 1993.2, with 3 different telescopes and 2 speckle camera systems. All of the 12 positive CHARA results have come from the Kitt Peak 4 m telescope.

Eight additional measurements of the system have been obtained by other speckle groups, and the 20 available measurements are listed in Table 1 along with the epochs at which no companion was detected. Data included in Table 1 are the epoch of observation expressed as the fractional Besselian year; the position angle θ uncorrected for precession; the angular separation ρ; the θ and ρ residuals to the orbit based solely upon the speckle data; telescope aperture; observed wavelength, when known; the relative weight given to the observation by the orbit solution to the speckle data based upon the precepts of Hartkopf *et al.* (1989); and a code for the original reference (the first three letters of the first author's name, plus the publication date). All of the data in Table 1 were obtained by the method of speckle interferometry except for the two observations by Ismailov (1992) which come from a phase grating interferometer. The estimated errors in the position angle and angular separation measurements of the CHARA data are $\pm 5\overset{\circ}{.}0$ and $\pm 10\%$, respectively. The errors are larger than we normally encounter, because of the small angular separation and large magnitude difference.

The "directed vector autocorrelation" reduction technique developed by Bagnuolo *et al.* (1992) allowed us to resolve the 180° ambiguity inherent in older speckle results, and to estimate a rough magnitude difference. The value of Δm for the two components was estimated to be approximately $\geqslant 2.0$ mag in the visual. The relatively large magnitude difference makes detection of the secondary extremely sensitive to seeing conditions. The predicted values of θ and ρ for the 35 epochs at which the secondary was not observed are shown in parentheses in Table 1. The 1977.3285 and 1985.2496 observations are the only two epochs for at which the system separation was definitely below the diffraction limit of resolution. The large Δm is responsible for the high proportion of negative results.

TABLE 1. Speckle interferometric observations of HR 6697.

Epoch (BY)	θ (°)	ρ (″)	$(O-C)_\theta$ (°)	$(O-C)_\rho$ (″)	Telescope (m)	λ (nm)	Relative Weight	Reference
1976.2965	339.9	0.110	-1.8	0.014	3.8	552	1.00	McA78
1976.3674	unresolved		(344.2)	(0.100)	2.1	552	0.00	HAR94
1976.5503	unresolved		(350.0)	(0.107)	2.1	552	0.00	HAR94
1976.6158	unresolved		(352.0)	(0.107)	2.1	552	0.00	HAR94
1976.6213	unresolved		(352.1)	(0.107)	2.1	552	0.00	HAR94
1977.3285	unresolved		(77.5)	(0.020)	2.1	552	0.00	HAR94
1977.4815	unresolved		(166.3)	(0.041)	3.8	552	0.00	McA81
1978.1474	unresolved		(294.6)	(0.042)	3.8	470	0.00	McA81
1978.1501	unresolved		(295.1)	(0.042)	3.8	470	0.00	McA81
1978.3169	unresolved		(318.5)	(0.059)	2.1	470	0.00	HAR94
1978.5382	unresolved		(334.2)	(0.082)	3.8	470	0.00	McA81
1978.6145	unresolved		(337.8)	(0.089)	3.8	470	0.00	McA81
1978.6174	unresolved		(337.9)	(0.089)	3.8	470	0.00	McA81
1979.1904	unresolved		(356.9)	(0.103)	2.1	470	0.00	HAR94
1979.3600	unresolved		(3.0)	(0.090)	3.8	470	0.00	McA81
1979.3626	unresolved		(3.1)	(0.089)	3.8	470	0.00	McA81
1979.529	unresolved		(12.9)	(0.064)	3.8	470	0.00	McA81
1980.477	unresolved		(275.2)	(0.037)	3.8	470	0.00	HAR84
1980.479	unresolved		(275.7)	(0.037)	3.8	470	0.00	HAR84
1980.482	unresolved		(276.5)	(0.037)	3.8	470	0.00	HAR84
1980.485	unresolved		(277.3)	(0.037)	3.8	400	0.00	HAR84
1980.720	unresolved		(317.4)	(0.058)	3.8	470	0.00	HAR84
1981.4706	350.8	0.098	-1.9	-0.009	3.8	470	1.00	McA84
1981.4732	351.8	0.114	-1.0	0.007	3.8	470	1.00	McA84
1981.7000	0.7	0.096	0.6	-0.001	3.8	470	1.00	McA84
1982.5028	unresolved		(193.1)	(0.052)	3.8	549	0.00	HAR94
1983.3072	330.3	0.063	-0.5	-0.013	6.0	600	0.25	BAL84
1983.3072	333.4	0.067	2.6	-0.009	6.0	656	0.25	BAL84
1983.4203	unresolved		(336.7)	(0.087)	3.8	549	0.00	HAR94
1983.7098	unresolved		(347.4)	(0.105)	3.8	549	0.00	HAR94
1984.2849	11.5	0.067	3.8	-0.010	6.0	600	0.25	BON85
1984.3668	unresolved		(13.6)	(0.062)	6.0	600	0.00	BAL85
1984.3759	unresolved		(14.4)	(0.060)	3.8	549	0.00	HAR94
1984.3840	21.8	0.065	6.6	0.007	3.8	549	1.00	HAR94
1984.8478	unresolved		(184.6)	(0.053)	6.0	600	0.00	BAL87
1985.2496	unresolved		(259.9)	(0.035)	1.9	550	0.00	BON85
1985.523	unresolved		(314.5)	(0.055)	3.6	549	0.00	McA87
1986.4052	355.1	0.093	-0.8	-0.012	6.0	600	0.25	BAL89
1986.4100	355.0	0.107	-1.1	0.002	3.8	549	1.00	HAR94
1986.4449	1.2	0.085	4.0	-0.018	3.6	700	0.25	BLA87
1986.6456	2.1:	0.066:	-2.8	-0.018	6.0	600	0.25	BAL89
1987.2728	unresolved		(185.9)	(0.053)	3.8	549	0.00	HAR94
1987.3832	unresolved		(199.8)	(0.050)	6.0	600	0.00	BAL89
1987.7617	unresolved		(285.2)	(0.039)	3.8	549	0.00	HAR94
1988.2612	338.2	0.085	1.0	-0.002	3.8	538	1.00	HAR94
1988.6655	349.1	0.101	-2.1	-0.006	3.8	549	1.00	HAR94
1989.2385	unresolved		(18.0)	(0.053)	3.8	549	0.00	HAR94
1989.3806	48.0	0.041	-12.8	0.019	1.0	550	0.25	ISM92
1989.4652	141.3	0.070	7.8	0.047	1.0	550	0.25	ISM92
1989.7084	183.3	0.067	-5.2	0.013	3.8	549	1.00	HAR94
1990.2733	unresolved		(303.9)	(0.047)	3.8	467	0.00	HAR94
1990.7542	347.0	0.093	6.5	-0.001	3.8	549	1.00	HAR94
1991.3193	358.1	0.098	-0.6	-0.002	3.8	549	1.00	HAR94
1992.3077	unresolved		(214.9)	(0.043)	3.8	549	0.00	HAR94
1993.2059	342.6	0.102	0.7	0.005	3.8	549	1.00	HAR94

2.2 Radial Velocities

The radial-velocity data for HR 6697 are presented in Table 2, which includes five new sets of velocities. The earliest set consists of 17 photographic spectrograms obtained by one of us (R.B.C.) with the coudé feed telescope and spectrograph system of Kitt Peak National Observatory (KPNO) between 1977 and 1982. Almost all of these spectrograms are of the blue region of the spectrum and have dispersions of 16.9 or 8.9 Å mm^{-1}. One spectrogram was taken of the red-wavelength region with a IIa-F plate at a dispersion of 17.6 Å mm^{-1}. The plates were measured with the Kitt Peak single coordinate Grant comparator, and the radial velocities were calculated with the computer facilities of the Colorado State University. Those data are designated "KPNO1" in Table 2.

Between 1986 and 1994, 25 spectroscopic observations were obtained by F.C.F. with KPNO's coudé feed telescope,

TABLE 2. Radial velocity data for HR 6697.

HJD -2400000.0	Phase	V_A ($km\,s^{-1}$)	$(O-C)_A$ ($km\,s^{-1}$)	Relative Weight	V_B ($km\,s^{-1}$)	$(O-C)_B$ ($km\,s^{-1}$)	Relative Weight	Source
30603.568	0.568	-26.2	0.6	0.00		(-42.0)		DDO
30885.812	0.888	-34.1	-4.9	0.00		(-38.3)		DDO
30963.542	0.976	-43.7	-2.8	0.00		(-20.5)		DDO
31282.642	0.339	-32.4	0.1	0.00		(-33.3)		DDO
31305.569	0.365	-36.4	-4.8	0.00		(-34.6)		DDO
31309.778	0.369	-33.3	-1.8	0.00		(-34.9)		DDO
43373.681	0.066	-49.3	-2.1	0.05		(-11.1)		KPNO1
43441.610	0.143	-39.3	3.0	0.05		(-18.4)		KPNO1
43582.009	0.303	-33.7	0.1	0.05		(-31.3)		KPNO1
43582.976	0.304	-35.0	-1.2	0.05		(-31.4)		KPNO1
43584.026	0.305	-34.7	-0.9	0.05		(-31.4)		KPNO1
43759.760	0.505	-30.6	-2.6	0.05		(-40.2)		KPNO1
43763.753	0.509	-27.9	0.0	0.05		(-40.3)		KPNO1
43764.772	0.510	-26.7	1.2	0.05		(-40.4)		KPNO1
44319.951	0.141	-41.0	1.5	0.05		(-18.2)		KPNO1
44502.650	0.348	-31.2	1.0	0.05		(-33.8)		KPNO1
44503.598	0.349	-30.9	1.3	0.05		(-33.9)		KPNO1
44504.615	0.350	-31.0	1.1	0.05		(-33.9)		KPNO1
44506.724	0.353	-31.1	0.9	0.05		(-34.0)		KPNO1
44685.951	0.556	-28.7	-1.7	0.05		(-41.7)		KPNO1
44803.838	0.690	-24.3	0.9	0.05		(-44.3)		KPNO1
44868.726	0.764	-20.1	5.1	0.00		(-44.5)		KPNO1
45020.013	0.935	-39.0	-4.6	0.05		(-30.5)		KPNO1
45491.804	0.471	-28.1	0.6	0.00		(-39.1)		Fick
46631.375	0.765	-25.2	0.0	0.50		(-44.5)		AAT
46638.328	0.773	-25.4	-0.2	0.50		(-44.4)		AAT
46718.564	0.864	-27.7	0.0	0.70		(-40.7)		KPNO2
46727.150	0.874	-28.7	-0.5	0.50		(-39.8)		AAT
46868.971	0.035	-47.1	0.3	0.70	-10.9	-0.2	0.02	KPNO2
46963.439	0.142	-42.6	-0.2	0.50		(-18.3)		AAT
46970.917	0.150	-41.7	0.1	0.70	-21.2	-2.0	0.02	KPNO2
46971.861	0.151	-41.7	0.1	0.70	-22.6	-3.3	0.02	KPNO2
46994.65	0.177	-39.9	0.2	1.00		(-21.8)		ESO
47008.385	0.193	-39.0	0.1	0.50		(-23.3)		AAT
47202.570	0.413	-29.6	0.6	0.50		(-36.8)		AAT
47232.72	0.448	-29.2	0.1	1.00		(-38.2)		H-P
47248.970	0.466	-29.4	-0.6	0.70		(-38.9)		KPNO2
47265.60	0.485	-29.5	-1.1	0.30		(-39.5)		Camb
47286.465	0.509	-27.5	0.4	0.50		(-40.3)		AAT
47309.867	0.535	-28.3	-0.9	0.70		(-41.1)		KPNO2
47315.51	0.542	-27.7	-0.5	0.30		(-41.3)		Camb
47358.43	0.590	-26.1	0.3	0.30		(-42.6)		Camb
47457.610	0.703	-25.3	-0.1	0.70	-45.4	-0.9	0.02	KPNO2
47468.28	0.715	-24.5	0.6	1.00		(-44.5)		H-P
47564.578	0.824	-25.8	0.3	0.50		(-43.1)		AAT
47615.70	0.882	-28.6	0.2	1.00		(-38.9)		H-P
47646.65	0.918	-31.9	0.2	1.00		(-34.0)		H-P
47673.452	0.948	-34.2	2.1	0.50		(-27.6)		AAT
47673.461	0.948	-36.0	0.3	0.50		(-27.6)		AAT
47673.53	0.948	-35.7	0.6	0.30		(-27.6)		Camb
47697.49	0.975	-40.9	-0.1	0.30		(-20.8)		Camb
47719.44	0.000	-44.2	0.4	0.30		(-15.0)		Camb
47744.41	0.028	-46.8	0.3	0.30		(-11.1)		Camb
47745.355	0.030	-47.2	0.0	0.50		(-11.0)		AAT
47791.262	0.082	-46.6	-0.2	0.50	-11.3	0.9	0.02	AAT
47809.593	0.103	-45.0	0.1	0.70	-15.5	-1.3	0.02	KPNO2
47810.589	0.104	-44.9	0.1	0.70	-13.5	0.8	0.02	KPNO2
47817.29	0.111	-44.4	0.1	0.30		(-15.1)		Camb
47832.25	0.128	-43.8	-0.5	1.00		(-16.9)		H-P
47918.75	0.226	-38.0	-0.7	1.00		(-26.1)		H-P
47963.98	0.278	-34.8	0.1	1.00		(-29.7)		DAO
47986.63	0.304	-33.6	0.2	0.30		(-31.3)		Camb
47991.490	0.309	-33.5	0.1	0.50		(-31.7)		AAT
48007.464	0.327	-32.4	0.5	0.50		(-32.7)		AAT
48012.57	0.333	-33.5	-0.8	0.30		(-33.0)		Camb
48020.333	0.342	-32.2	0.2	0.50		(-33.5)		AAT
48031.422	0.354	-31.7	0.3	0.50		(-34.1)		AAT
48056.834	0.383	-30.7	0.4	0.70		(-35.5)		KPNO2
48074.410	0.403	-30.6	-0.1	0.50		(-36.4)		AAT
48075.52	0.404	-30.1	0.3	0.30		(-36.5)		Camb
48105.362	0.438	-29.8	-0.3	0.50		(-37.8)		AAT
48151.328	0.491	-29.4	-1.1	0.50		(-39.7)		AAT
48167.632	0.509	-28.0	-0.1	0.70		(-40.3)		KPNO2
48171.35	0.513	-27.8	0.0	0.30		(-40.5)		Camb
48232.22	0.582	-26.1	0.4	0.30		(-42.4)		Camb
48284.75	0.642	-25.2	0.5	1.00		(-43.7)		H-P
48346.955	0.713	-25.6	-0.5	0.70	-45.5	-1.0	0.02	KPNO2
48349.463	0.715	-24.8	0.3	0.50		(-44.5)		AAT
48372.509	0.742	-25.6	-0.5	0.50		(-44.6)		AAT
48385.56	0.756	-25.1	0.0	0.30		(-44.5)		Camb
48418.55	0.794	-25.8	-0.3	0.30		(-44.0)		Camb
48427.816	0.804	-25.0	0.6	0.70	-44.9	-1.1	0.02	KPNO2
48448.338	0.828	-26.3	-0.1	0.50		(-42.9)		AAT
48453.45	0.834	-27.1	-0.7	0.30		(-42.6)		Camb
48456.43	0.837	-25.6	0.9	0.30		(-42.5)		Camb
48460.365	0.841	-27.1	-0.5	0.50		(-42.2)		AAT
48505.672	0.893	-29.4	0.2	0.70		(-37.7)		KPNO2
48559.23	0.954	-37.5	-0.3	1.00		(-26.3)		H-P
48577.555	0.974	-40.4	0.2	0.70	-21.5	-0.5	0.02	KPNO2
48578.587	0.976	-41.0	-0.2	0.70	-19.9	0.8	0.02	KPNO2
48604.552	0.005	-46.4	-1.2	0.70	-14.2	-0.1	0.02	KPNO2
48605.553	0.006	-46.0	-0.7	0.70	-13.8	0.1	0.02	KPNO2

TABLE 2. (continued)

HJD -2400000.0	Phase	V_A (km s^{-1})	(O-C)$_A$ (km s^{-1})	Relative Weight	V_B (km s^{-1})	(O-C)$_B$ (km s^{-1})	Relative Weight	Source
48606.546	0.007	-45.6	-0.1	0.70	-14.1	-0.4	0.02	KPNO2
48608.21	0.009	-46.0	-0.3	1.00		(-13.4)		H-P
48642.76	0.048	-47.4	0.2	1.00		(-10.5)		H-P
48680.07	0.091	-45.5	0.4	1.00		(-13.0)		DAO
48736.64	0.155	-41.4	0.1	1.00		(-19.7)		H-P
48738.443	0.157	-41.0	0.4	0.50	-13.7	6.0	0.00	AAT
48770.920	0.194	-38.5	0.6	0.70		(-23.4)		KPNO2
48772.832	0.196	-38.8	0.1	0.70	-22.2	1.3	0.02	KPNO2
48800.55	0.228	-37.2	0.0	1.00		(-26.2)		H-P
48848.41	0.282	-34.6	0.1	1.00		(-30.0)		H-P
48914.623	0.357	-31.8	0.1	0.70		(-34.3)		KPNO2
48975.21	0.426	-29.8	0.0	1.00		(-37.4)		H-P
49036.70	0.496	-28.0	0.2	1.00		(-39.9)		H-P
49071.66	0.535	-27.3	0.1	1.00		(-41.1)		H-P
49104.016	0.572	-26.7	0.0	0.70	-44.8	-2.7	0.02	KPNO2
49176.56	0.655	-25.3	0.3	1.00		(-43.9)		H-P
49242.38	0.729	-24.8	0.3	1.00		(-44.6)		H-P
49245.607	0.733	-24.8	0.3	0.70		(-44.6)		KPNO2
49250.589	0.739	-24.9	0.2	0.70		(-44.6)		KPNO2
49355.75	0.858	-27.4	0.0	1.00		(-41.1)		H-P
49404.73	0.914	-31.9	-0.3	1.00		(-34.7)		H-P
49475.61	0.994	-44.1	-0.4	1.00		(-16.3)		H-P

coudé spectrograph, and a Texas Instruments CCD detector. Most of the observations were centered at 6430 Å, although three spectra were obtained of the lithium region at 6708 Å. All these observations cover a wavelength range of 80 Å and have a resolution of 0.2 Å. Most velocities were determined relative to μ Her A, a G5 IV star with an assumed velocity of -16.4 km s^{-1}. The velocity was determined by Stockton & Fekel (1992) relative to the International Astronomical Union (IAU) velocity standard β Oph (Scarfe *et al.* 1990). Several observations were reduced relative to the IAU velocity standards ι Psc, HR 7560, or β Vir, whose velocities have been assumed from the work of Scarfe *et al.* (1990). Fekel *et al.* (1978) have given the general details of the reduction procedure. In addition to the lines of the solar-type primary, very weak lines from the secondary are visible in the red-wavelength CCD spectra (Fig. 1). At most orbital phases the line profiles of the two stars are completely or partially blended; nevertheless, radial velocities of both components could in many cases be determined with the IRAF cross-correlation program FXCOR that uses two Gaussians to fit the blended profiles. A total of 15 velocities of the secondary has been obtained. Those observations are designated "KPNO2" in Table 2.

A third set of 24 observations, including one measurement of the velocity of the secondary, was obtained by A.A.T. (designated "AAT" in Table 2) between 1986 and 1992. The observations were taken at different telescopes ranging from 0.6 to 1.0 m at different observatories, but mostly in Crimea and in Moscow with a correlation radial-velocity meter similar to *CORAVEL*. Tokovinin (1987) discussed this radial-

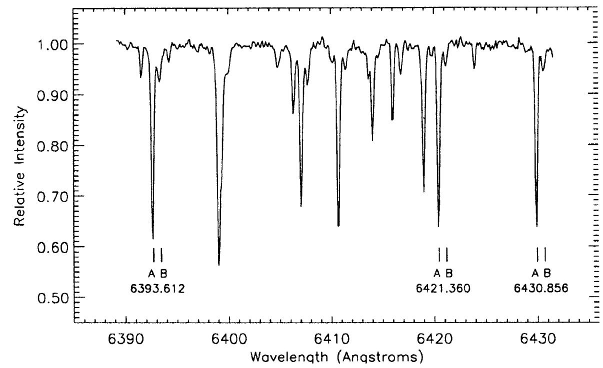

FIG. 1. A region of the red-wavelength spectrum of HR 6697 is shown with three identified double-lined features.

velocity instrument and the velocity reductions.

Beginning in 1987, 41 radial-velocity measurements were obtained by R.F.G. Seventeen were with the original radial-velocity spectrometer at Cambridge (Griffin 1967) while 21 were with the Geneva Observatory's *CORAVEL* at Haute-Provence (Baranne *et al.* Poncet 1979) and one with a similar instrument at the European Southern Observatory. Those 39 observations comprise the fourth and fifth datasets, and are designated "Camb," "H–P," and "ESO," respectively. Two additional velocities, obtained by R.F.G. with the radial-velocity spectrometer at the Dominion Astrophysical Observatory (Fletcher *et al.* 1982), are designated "DAO" in Table 2.

The five sets of observations plus the two DAO velocities, the old observations obtained at David Dunlap Observatory ("DDO") by Young (1945), and one recent observation from Fick Observatory (Beavers & Eitter 1986; designated "Fick") results in a total of 114 velocities for the primary and 17 velocities for the secondary; these are listed in Table 2. Also included in Table 2 are the heliocentric Julian date; the orbital phase; velocity, velocity residual, and relative weight in the spectroscopic orbit solution for the A and B components; and the source of the observation. For those observations where no B component was measured, the predicted velocity is given in parentheses.

The phases and velocity residuals in Table 2 were calculated from an orbit based upon a joint solution of the speckle and radial velocity data. The solution is described in Sec. 3. Average residuals (in km s^{-1}) from the five primary datasets are

$$\mathrm{rms}_{\mathrm{KPNO1}} = -0.18 \pm 2.19;$$

$$\mathrm{rms}_{\mathrm{KPNO2}} = -0.04 \pm 0.43;$$

$$\mathrm{rms}_{\mathrm{AAT}} = +0.08 \pm 0.57;$$

$$\mathrm{rms}_{\mathrm{Camb}} = +0.00 \pm 0.51;$$

and

$$\mathrm{rms}_{\mathrm{H-P+ESO}} = +0.03 \pm 0.32.$$

The residuals show no significant systematic offsets, but they do demonstrate the improvement afforded by modern meth-

TABLE 3. Results of McCormick astrometric study.

without orbital terms:		
π_X	=	0″0336 ± 0″0032
π_Y	=	0″0345 ± 0″0138
with orbital terms:		
π_X	=	0″0344 ± 0″0031
π_Y	=	0″0295 ± 0″0116
π_{rel}	=	0″0341 ± 0″0030
π_{abs}	=	0″0379 ± 0″0030
μ_X	=	-0″0125 ± 0″0004 yr^{-1}
μ_Y	=	0″0767 ± 0″0005 yr^{-1}

ods. The CCD and velocity meter results have standard deviations five times smaller than the photographic results.

2.3 *Astrometry*

A parallax and proper motion for HR 6697 were first published by Ianna *et al.* (1990) based on 75 Kodak 103a-G plates containing 235 images obtained between 1974.3 and 1982.7 with the McCormick 67 cm photovisual refractor. To reduce the brightness of the parallax star to that of the reference star background, it was observed through a GG 495 filter upon which had been deposited an Inconel spot, 1 cm in diameter, of photographic density 2.0. This procedure avoids the problems that may arise from using narrow slits in rotating sectors to achieve large-magnitude attenuations. The plates were measured manually on the Observatory's two-coordinate Grant comparator, and standard McCormick procedures (Ianna 1979) were followed.

The astrometric material was subsequently expanded by obtaining 8 additional plates centered around 1992.5. The best 53 plates of HR 6697 were then measured on the McCormick PDS 1010GM. The machine has laser interferometer stage encoders, and although we now have used just 161 images from 22 nights, the PDS measurements yield results with somewhat higher precision. The final relative parallax and proper motions based on an iterative central-overlap solution are summarized in Table 3. The values supercede the earlier ones and are adopted here; the influence of the binary orbit is discussed in Sec. 3.

From microdensitometer scans with the Mount Stromlo PDS 1010A of two plates with six exposures and photoelectric photometry of two of the reference stars, we have determined the apparent visual magnitude of the reference stars; their mean magnitude is +10.8. From van Altena (1974) the mean parallax of the reference stars is taken to be 0″0038, which then corrects our relative parallax to an absolute one.

A subset of the plate material covering the full time interval of the data was remeasured on the PDS to include six stars in the field with proper motions in the PPM catalog. The six stars were used to find a correction to adjust our relative proper motion for HR 6697 to the system of the FK5. The derived absolute motions are listed in Table 3; they are in good agreement with the PPM values for HR 6697 and have higher accuracy.

TABLE 4. Observed and computed colors of HR 6697.

V	$U-B$	$B-V$	$b-y$	$V-R$	$R-I$	Reference or Model
6.305	0.201	0.659		0.537	0.328	Fernie 1981
6.293		0.642		0.567	0.364	Parsons & Montemayor 1982
6.30		0.626				Haggkvist & Oja 1987
6.328			0.413			Sowell & Wilson 1993
6.35	0.18	0.65		0.55	0.36	This paper
6.315	0.19	0.64	0.413	0.55	0.35	Average
	0.10	0.57	0.361	0.49	0.32	F8 V + K0 V, $\Delta m_V = 2.0$
	0.09	0.57	0.368	0.50	0.31	F8 V + K2 V, $\Delta m_V = 2.5$
	0.16	0.63	0.392	0.53	0.34	G0 V + K0 V, $\Delta m_V = 1.5$
	0.16	0.63	0.390	0.54	0.34	G0 V + K2 V, $\Delta m_V = 2.0$
	0.14	0.62	0.389	0.54	0.34	G0 V + K3 V, $\Delta m_V = 2.5$
	0.13	0.62	0.384	0.53	0.35	G0 V + K5 V, $\Delta m_V = 3.0$
	0.20	0.67	0.418	0.56	0.36	G2 V + K2 V, $\Delta m_V = 2.0$
	0.20	0.66	0.414	0.58	0.38	G2 V + K5 V, $\Delta m_V = 2.5$

2.4 *Photometry*

The V magnitude and colors of HR 6697 were obtained by P.A.I. from one night's photometry in 1981 at the Kitt Peak National Observatory 0.45 m reflector, using an RCA 31034 photomultiplier and Kron–Cousins filter set as recommended by Bessell (1979). Cousins equatorial standards were measured and used for estimating extinction and transformation coefficients. The residuals for the standard star observations for the night gave a standard error in V of ±0.025 mag and of ±0.01 mag or less in each of the colors. The V mag and colors are listed in Table 4, along with other magnitudes and colors for HR 6697 found in the literature, where $(V-R)_c=0.51$ and $(V-I)_c=0.71$ have been converted to the Johnson system with the equations of Bessell (1979).

Sowell & Wilson (1993) obtained photometric observations of HR 6697 in 1989 and 1991 from which Strömgren colors and indices were calculated as well as the V magnitude. Their results were $V=+6.328\pm0.008$, $(b-y)=+0.413\pm0.003$, $m_1=+0.203\pm0.005$, and $c_1=+0.371\pm0.008$. The color indices include light from both components and fit the calibration relations established by Olsen (1984) without showing evidence of evolution.

3. ORBITAL ANALYSES

The spectroscopic and speckle datasets cover 21 and 7 orbital revolutions, respectively. The velocity coverage for the primary component is excellently distributed over phase, however, the (θ,ρ) distribution is far less favorably distributed. For these reasons, we followed the approach of first calculating an independent spectroscopic orbit, and then adopting the spectroscopically determined P, T, and e for the calculation of the "visual" orbit from the speckle data.

For comparison's sake, an independent orbit based only on speckle data was also computed. A fourth orbital solution was carried out using the two data types in a combined solution. The orbital motion has also been detected in the astrometric data.

To derive preliminary spectroscopic orbital elements, the method of Lehmann–Filhes (Aitken 1964) was used on a subset of the data. The elements were improved with a differential corrections program (Barker *et al.* 1967), then orbital solutions of the primary were obtained for each of the five datasets mentioned previously. From these results zero-point corrections were applied: -0.2 km s^{-1} was added to the velocities of Tokovinin; -0.4 km s^{-1} to Griffin's Cambridge velocities; and -0.6 km s^{-1} to Griffin's *CORAVEL* velocities. No zero-point corrections were applied to any of the other velocities. From the variances of the above solutions, unit weights were assigned to Griffin's *CORAVEL* velocities, 0.7 to Fekel's KPNO velocities, 0.5 to Tokovinin's, 0.3 to Griffin's Cambridge velocities, and 0.05 to Culver's. A solution of the primary then was obtained with all five datasets included, and resulted in a period of 879.9 days. Addition of the old DDO velocities significantly extends the time baseline and might be expected to improve the period. When included in an orbital solution, they resulted in a period increase of 1–2 days depending on the weights assigned to them but also required a zero-point shift of $2\text{–}3 \text{ km s}^{-1}$ to produce a mean residual close to zero. We have considered the DDO velocities to be marginal at best and have given them zero weight in the final solution, although the uncorrected velocities and their residuals are listed in Table 2.

Finally, a simultaneous solution of both components was determined with the secondary velocities given weights of 0.02. In this final spectroscopic solution the lone Fick velocity and one photographic-plate velocity have been given zero weight (see Table 2). The orbital elements of this double-lined solution are listed in Table 5.

The elements of the visual orbit were then found by adopting the spectroscopic elements P, T, and e and performing a solution using the "grid search" algorithm described by Hartkopf *et al.* (1989) for the geometric elements i, a'', ω, and Ω from the speckle observations. The new elements are included in Table 5 under "speckle solution I" and show that the orbit has a relatively high inclination, as a result of which the system can be expected to be unresolved with 4 m class telescopes through portions of its orbit. The element ω, which is defined with a 180° difference between spectroscopic and visual values, is the only element determined independently in these two solutions. The difference in the two results is expected to be small owing to the relatively large eccentricity, and, indeed, the spectroscopic and speckle values differ by only 0°.3, attesting to the compatibility of the two data types.

When the orbit is determined only from the speckle data (Table 5, "speckle solution II"), the lack of uniform coverage yields a significantly lower eccentricity. The rms residuals ($\sigma_{\Delta\rho}$, $\sigma_{\rho\Delta\theta}$) for speckle solutions I and II are (±0″.0072, ±0″.0044) and (±0″.0071, ±0″.0040). The modest decrease in the residuals from the speckle-only case does not argue strongly against adopting the spectroscopic P, T, and

TABLE 5. Orbital elements of HR 6697.

Element	Spectroscopic Solution	Speckle SolutionI	Speckle Solution II	Combined Solution
P (days)	879.88 ± 0.70	879.88 *	880.7	880.78 ± 0.83
P (yr)	2.4090 ± 0.0019	2.4090 *	2.411	2.4115 ± 0.0023
T (HJD)	47718.68 ± 1.51	47718.68 *	47729.9	47719.3 ± 2.2
T (BY)	1989.525 ± 0.004	1989.525 *	1989.555	1989.527 ± 0.006
a'' (arcsec)		0.084	0.086	0.085 ± 0.002
i (°)		68.5	69.7	68.1 ± 1.5
Ω (°)		178.6	176.1	178.4 ± 1.7
e	0.4298 ± 0.0048	0.4298 *	0.364	0.423 ± 0.007
ω (°) †	136.76 ± 0.88	317.1	322.2	317.2 ± 1.2
K_A (km s^{-1})	11.288 ± 0.072			11.24 ± 0.12
K_B (km s^{-1})	16.98 ± 0.63			17.06 ± 0.77
γ (km s^{-1})	−32.800 ± 0.045			−32.83 ± 0.07
$a_A \sin i$ (km)	$(123.3\pm0.9)\times10^6$			$(123.4\pm1.4)\times10^6$
$a_B \sin i$ (km)	$(185.5\pm7.0)\times10^6$			$(187.2\pm8.5)\times10^6$
$M_A \sin^3 i$ ($M_\odot$)	0.913±0.070			0.930±0.093
$M_B \sin^3 i$ ($M_\odot$)	0.607±0.026			0.613±0.036

† value for component A in spectroscopic solution, component B in other solutions

* elements adopted from spectroscopic solution

e. The orbital period from the speckle solution II is 0.09% longer than the spectroscopic period and periastron is predicted to occur 11 days later or 4°.6 in phase later. On the whole, the independent solutions from the two data types are in remarkably good agreement. A visual orbit has recently been published by Baize (1994), and his visual elements are in reasonable agreement with those determined here.

Finally, we determined a simultaneous solution of all the radial velocity and speckle data (Table 5) with an interactive program developed by one of us (A.A.T.) that computes all ten orbital elements with the least-squares method. Tokovinin (1992) gives a summary of some of the useful features of this program. The results from that solution are presented in the last column in Table 5, and we adopt those elements as definitive for the orbit of HR 6697. Radial velocities and speckle observations are plotted together with curves predicted by these elements in Figs. 2 and 3, respectively.

The large Δm of the system and the orbital semimajor axis from the speckle observations open the possibility for substantial influence on the parallax and proper motion by the orbital motion of the image photocenter. For $\Delta m \sim 2.8$ mag, the photocentric motion will be about 33% that of the motion of the binary (van de Kamp 1967). The photocentric semimajor axis would be expected to be approximately 0″.028. Figure 4 shows the photocentric motion predicted from the orbital elements in Table 5 along with nightly mean residuals from the parallax solution. The orbital motion is especially apparent in the Y residuals.

With this in mind, a new parallax and proper motion solution was carried out including orbital terms calculated from the final orbital elements derived from the spectroscopic and speckle data. Small changes in the X (i.e., RA) and Y (Dec) parallaxes occur and the error in the y parallax shows a small reduction with the addition of the orbital terms (Table 3). The

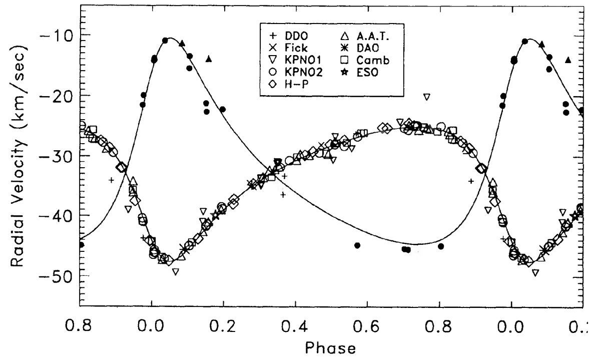

FIG. 2. The observed velocities are shown plotted against the combined speckle/spectroscopic orbit. Open symbols are for the primary and filled symbols are for the secondary.

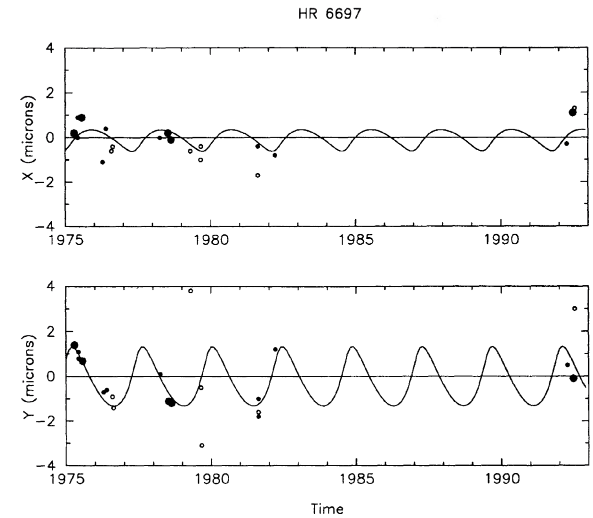

FIG. 4. Time displacement curves for the motion of the HR 6697 photocenter in right ascension (X) and declination (Y). The plotted points are the nightly residuals from the parallax solution. Open circles represent points with $\sigma\sim1.5$ μm, filled circles have $\sigma\sim1.0$ μm, and large solid points have $\sigma\sim0.5$ μm. One μm corresponds to 0\".020.

photocentric semimajor axis found in this solution is $\alpha=0\overset{\prime\prime}{.}0289\pm0\overset{\prime\prime}{.}0032$. It is of interest to compare this result with the angular semimajor axis a'' of Table 5. From α, the Δm for the system and the fractional mass (van de Kamp 1967), we calculate a semiaxis major of 0\".088, in excellent agreement with the speckle result.

4. DISCUSSION

4.1 Spectral Types and Masses

The direct resolution of a double-lined spectroscopic binary enables the determination of the individual masses of the components and the distance to the system to be made by combining the angular information from the speckle data with the linear information from the velocities. The combined orbital solution permits the determination of an "orbital parallax" from the relation

$$\pi_{\text{orb}}=\frac{1.496\times10^8\times a''\times\sin i}{a_A\ \sin i+a_B\ \sin i},$$

where the quantities in the numerator come from the speckle data, and those in the denominator from the radial velocities. From this equation, we calculate $\pi_{\text{orb}}=0\overset{\prime\prime}{.}0.375\pm0\overset{\prime\prime}{.}0014$ corresponding to a distance of 26.7 ± 1.0 pc, in remarkable agreement with the trigonometric parallax $\pi_{\text{trig}}=0\overset{\prime\prime}{.}0379\pm0\overset{\prime\prime}{.}0030$ (or $d=26.4\pm2.1$ pc). The weighted mean average of these two independent measures of the parallax is $\langle\pi\rangle=0\overset{\prime\prime}{.}0376\pm0\overset{\prime\prime}{.}0013$, leading to a distance $d=26.6\pm0.9$ pc and a distance modulus $m-M=2.124\pm0.073$ mag. HR 6697 thus falls just outside the range of distances of the "nearby stars" as defined by Woolley *et al.* (1970).

The speckle observations provide the orbital inclination $i=68\overset{\circ}{.}1\pm1\overset{\circ}{.}5$, which, when combined with the spectroscopically determined quantities $m_{A,B}\sin^3 i$, yields masses of $m_A=1.16\pm0.12\ \mathcal{M}_\odot$ and $m_B=0.77\pm0.05\ \mathcal{M}_\odot$. To reduce the errors in the masses significantly would require improved values for $K_{A,B}$ and i with the greatest gain from reducing the uncertainty in K_B.

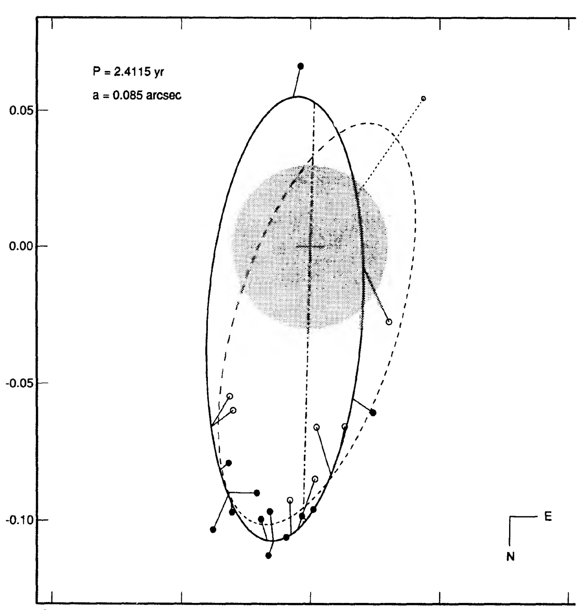

FIG. 3. The speckle interferometric measurements are shown plotted against the combined speckle/spectroscopic solution. The dashed curve indicates the orbit of Baize (1994).

In an attempt to determine the spectral types of the individual components, the spectrum addition technique of Strassmeier & Fekel (1990) was used. They identified several luminosity-sensitive and temperature-sensitive line ratios in the 6430–6465 Å region and used them, along with the general appearance of the spectrum, as spectral-type criteria. Since the comparison is done by trial and error, previous spectral classifications are important as a starting point.

The primary star's spectrum was first compared with that of the Sun. The critical line ratios of 6432 Å/6430 Å and

6456 Å/6455 Å indicate that the primary of HR 6697 has an earlier spectral type. In addition, the diluted lines of the primary are stronger than those of the Sun, indicating that HR 6697 has a higher metallicity. The spectrum was then compared with HR 483 (G1.5 V; Keenan & McNeil 1989) and β Vir (F9 V; Morgan & Keenan 1973), both of which are somewhat metal rich ([Fe/H]=0.1–0.2) according to the references in Cayrel de Strobel *et al.* (1992). The critical line ratios suggest a spectral type for the primary of G0 V with an uncertainty of one subclass. Because of the large-magnitude difference between the components, the lines of the secondary are extremely weak and, thus, its spectral type is significantly more difficult to determine. Furthermore, except for HR 511 (K0 V; Morgan *et al.* 1953) none of our K dwarf reference stars is metal rich. Stars with spectral types between K0 V and K5 V give similar fits to the spectrum of the secondary although in all cases the lines are not deep enough presumably because most of the K stars are not metal rich. Because the K0 V reference star is metal rich, the spectral type of the secondary is probably somewhat later than that. On the basis of these line ratios, we estimate spectral types of G0 V and K3 V for the two components.

The magnitude difference of the stars was determined from our spectra of the 6430 Å region. The mean line depth ratio, B/A, of three moderate-strength Fe I lines in this region was found to be 0.13. To determine the magnitude difference, this ratio must be corrected for the increased line strength of the secondary. This effect was estimated by determining the mean ratio of the line strengths of the same lines in the reference stars HR 483 (G1.5 V) and HR 8832 (K3 V; Keenan & McNeil 1989). We estimate the luminosity ratio as 0.13×0.74 or 0.096, which corresponds to a magnitude difference of 2.54 at 6430 Å. Such a wavelength is about 0.6 of the way between the Johnson V and R bandpasses. From an examination of $(V-R)$ colors (Johnson 1966) the V magnitude difference is estimated to be 2.8±0.3 mag.

Mason (1994) has shown from a comparison of speckle and occultation binaries that we are capable of detecting Δm's as large as 3 mag under average seeing conditions by speckle interferometry. The value $\Delta m \sim 2.8$ is close to our limit of detectability, and it is not surprising that the system is frequently unresolved.

The observed colors of the system also enable us to estimate the spectral types of the components and an approximate magnitude difference. Colors in the Johnson system have been obtained by Fernie (1981), Parsons & Montemayor (1982), and Haggkvist & Oja (1987). Their colors along with our values, which have been transformed to the Johnson system, are listed in Table 4. To obtain the observed colors of the system, a spectral type close to solar was assumed for the primary. From the spectral type versus color relation of Johnson (1966) and various assumed magnitude differences, several models of the combined colors have been computed, the best of which are listed for comparison in Table 4. Spectral-type combinations of (G0 V+K0 V or K2 V) as well as (G2 V+K2 V) appear to reproduce the observed average wideband colors quite well. The combination of (G0 V+K3 V) with a magnitude difference of 2.5 in V appears to be acceptable except perhaps in the U bandpass.

TABLE 6. Derived properties for HR 6697.

M_A	=	$1.16 \pm 0.12\ M_\odot$
M_B	=	$0.77 \pm 0.05\ M_\odot$
$\log(M_A/M_\odot)$	=	$+0.066 \pm 0.045$
$\log(M_B/M_\odot)$	=	-0.115 ± 0.028
d	=	26.6 ± 0.9 pc
$m-M$	=	$+2.124 \pm 0.073$ mag
M_{VA}	=	$+4.27 \pm 0.10$ mag
M_{VB}	=	$+7.07 \pm 0.32$ mag
L_A	=	$1.61 \pm 0.15\ L_\odot$
L_B	=	$0.17 \pm 0.05\ L_\odot$
$\log(L_A/L_\odot)$	=	$+0.208 \pm 0.040$
$\log(L_B/L_\odot)$	=	-0.768 ± 0.128

The $(b-y)$ color obtained by Sowell & Wilson (1993) can similarly be used as a basis for determining the individual spectral types and Δm by means of the calibration of $(b-y)$ versus spectral type for luminosity class V stars of Ardeberg & Lindgren (1985). In this instance, the Strömgren color is best matched by the combination (G2 V+K5 V) and would permit an even later spectral type for the secondary. This combination matches $(U-B)$ quite well.

The spectral type combination in Table 4 that gives the smallest mean deviation overall from the five colors is (G2 V+K2 V). However, because the spectral line analysis indicates a primary earlier than the Sun, we conclude that the spectral types are in the range G0 to G2 for the primary and K2 to K5 for the secondary in the sense that the later the subclass of the primary the later the subclass for the secondary. The mass ratio $m_A/m_B=1.50\pm0.05$ could potentially resolve this issue further if the derived errors in the masses were smaller and if the spectral type versus mass relation possessed smaller intrinsic scatter. Although the mass ratios for these spectral types as taken from Allen (1973) do not help discriminate spectral types further, it is worth noting that our mass ratio is completely consistent with what is anticipated by existing data.

We conclude on the basis of spectral line depth ratios (which is given the greatest weight), speckle interferometry, and likely spectral types that $\Delta m=2.8\pm0.3$ mag. Combining this with the mean distance of 26.6±0.9 pc and the mean V magnitude, we find absolute magnitudes for the components of $M_{VA}=+4.27\pm0.10$ and $M_{VB}=+7.07\pm0.32$. Applying bolometric corrections of -0.04 and -0.40 for the G and K stars, respectively, (Allen 1973), we find $L_A=1.61\pm0.15L_\odot$ and $L_B=0.17\pm0.05L_\odot$. Table 6 contains a summary of the derived physical parameters for the components of HR 6697.

A consistency check on spectral types, masses, and luminosities is provided by a comparison with known G and K masses. Our values of 1.16±0.12 $\mathscr{M}_\odot$ and 0.77±0.05 $\mathscr{M}_\odot$ would appear to be somewhat larger than the canonical values listed in Allen (1973). However, work over the past 15 yr on K dwarfs (Griffin 1978; Griffin *et al.* 1982; Fekel & Beavers 1984; Griffin *et al.* 1985) as well as the masses (about half of which are preliminary values) of the G and K main-sequence components listed by Popper (1993) suggest that the masses are consistent with our spectral classifications. When our new results for HR 6697 are overlaid on the theoretical $\log m$ vs $\log L$ diagram shown as Fig. 8 of Popper *et al.* (1986), the primary component falls on the $\log t=9.2$ isochrone. The A and B components provide a slope for this relation of $\Delta \log L/\Delta \log m=5.4\pm1.8$, consistent with the models but lacking in sensitivity due to the relatively large errors in the masses. HR 6697 is listed in the Bright Star Catalogue (Hoffleit & Jaschek 1982) as having spectral type G2V, probably based upon the classification of Harlan & Taylor (1970), and thus could reasonably be assumed to be a candidate for a solar analog (Neckel 1986). We find, however, that the primary component is somewhat more massive and significantly more luminous than the sun.

With our center of mass velocity (Table 5), proper motions (Table 3), and distance of 26.6 pc, the U,V,W space velocities are -27, -19, and -7 km s^{-1}, respectively. Comparison with the various moving groups listed by Soderblom & Mayor (1993) suggests that it is not a member of any of them, although the V component of the Hyades moving group is -16 km s^{-1}. However, as noted by Soderblom & Mayor (1993), members of a moving group must have virtually identical V motions.

4.2 Lithium Abundance and Age

The measured equivalent width of the lithium line in HR 6697 A, the early G dwarf component, is 19 mÅ. After correcting for the continuum of the companion, the equivalent width is 21 mÅ. To convert the equivalent width to an abundance, we have assumed T_e=5850 K, a temperature slightly hotter than the solar value and consistent with a G1 V spectral type. Interpolating in Table 2 of Soderblom *et al.* (1993) results in $\log \epsilon(\mathrm{Li})=1.93$. Because lithium is easily ionized, this value is most sensitive to the assumed T_e; a change of 100 K results in a change of ±0.1 in the log abundance.

Work over the past 15 yr has confirmed that the main-sequence lithium-depletion rate depends on the mass of the star but it has also shown that at least one unknown additional parameter affects the depletion rate of population I dwarfs. The situation recently has been extensively reviewed by Soderblom *et al.* (1993). While in many instances lithium may not be a good quantitative indicator of age, Pallavicini *et al.* (1987) have shown that it can be useful as a qualitative discriminator.

The Hyades is a relatively young metal-rich cluster with an age of 6×10^8 yr. The results of Cayrel *et al.* (1984) indicate that a Hyad of similar temperature to HR 6697 A has a lithium equivalent width of about 65 mÅ and a log lithium abundance of 2.5. The abundance of lithium in HR 6697 A compared to that in similar Hyades stars suggests that HR 6697 is significantly older than the Hyades and so somewhat evolved from the zero-age main sequence. Such an age is consistent with the narrow lines of the spectrum and thus the slow rotation of the star. It also supports our conclusion from the mass and luminosity of the primary that it has significantly evolved from the ZAMS.

We wish to thank Dr. Helmut Abt of KPNO for so generously obtaining two of the spectrograms listed in Table 1. We thank Mary Morton for measuring several of the KPNO CCD spectrograms. The parallax program at the Leander J. McCormick Observatory is partially supported by the National Science Foundation, most recently through Grant No. AST 90-16686, and the Estate of Leander J. McCormick. The speckle interferometry program at Georgia State University has been supported by the National Science Foundation, most recently through Grant No. AST 94-16994, by the Office of the Dean of the College of Arts and Sciences and by the Chancellor's Initiative Fund administered by the Office of the Vice President for Research and Information Technology at GSU. F.C.F.'s research has been supported in part by NASA Grant No. NAG8-1014 to TSU.

REFERENCES

Aitken, R. G. 1964, The Binary Stars (Dover, New York), p. 138
Allen, C. W. 1973, Astrophysical Quantities, 3rd ed. (Athlone Press, London)
Ardeberg, A., & Lindgren, H. 1985, in Calibration of Fundamental Stellar Quantities, IAU Symposium No. 111, edited by D. S. Hayes, L. E. Pasinetti, and A. G. Davis Philip (Reidel, Dordrecht), p. 509
Bagnuolo, Jr., W. G., Mason, B. D., Barry, D. J., Hartkopf, W. I., & McAlister, H. A. 1992, AJ, 103, 1399
Baize, P. 1994, A&AS, 106, 267
Balega, I. I., & Balega, Y. Y. 1987, SvAL, 13, 208 (BAL87)
Balega, I. I. Balega, Yu. Yu., & Vasyuk, V. A. 1989, Astrofiz. Issled. Izv. Spets. Astrofiz. Obs. 28, 107 (BAL89)
Balega, Y. Y., & Balega, I. I. 1985, SvAL, 11, 47 (BAL85)
Balega, Y. Y., & Ryadchenko, V. P. 1984, SvAL, 10, 95 (BAL84)
Barker, E. S., Evans, D. S., & Laing, J. D. 1967, R. Obs. Bull., 130
Baranne, A., Mayor, M., & Poncet, J.-L. 1979, Vistas Astron., 23, 279
Beavers, W. I., & Eitter, J. J. 1986, ApJS, 62, 147
Bessell, M. S. 1979, PASP, 91, 589
Blazit, A., Bonneau, D., & Foy, R. 1987, A&AS, 71, 57 (BLA87)
Bonneau, D., Balega, Y. Y., Blazit, A., Foy, R., Vakili, F., & Vidal, J. L. 1985, A&AS, 65, 27 (BON85)
Cayrel, R., Cayrel de Strobel, G., Campbell, B., & Däppen, W. 1984, ApJ, 283, 205
Cayrel de Strobel, G., Hauck, B., Francois, P., Thévenin, F., Friel, E., Mermilliod, M., & Borde, S. 1992, A&AS, 95, 273
Culver, R. B., Ianna, P. A., & McAlister, H. A. 1981, BAAS, 12, 850
Fekel, F. C., & Beavers, W. I. 1984, ApJ, 267, 682
Fekel, F., Bopp, B. W., & Lacy, C. H. 1978, AJ, 83, 1445
Fernie, J. D. 1981, ApJ, 243, 576
Fletcher, J. M., Harris, H. C., McClure, R. D., & Scarfe, C. D. 1982, PASP, 94, 1017
Griffin, R. F. 1967, ApJ, 148, 465
Griffin, R. F. 1978, Observatory, 98, 257

Griffin, R. F., Gunn, J. E., Zimmerman, B. A., & Griffin, R. E. M. 1985, AJ, 90, 609
Griffin, R. F., Mayor, M., & Gunn, J. E. 1982, A&A, 106, 221
Haggkvist, L., & Oja, T. 1987, A&AS, 68, 259
Halliwell, M. 1981, ApJS, 47, 243
Harlan, E. A. & Taylor, D. C. 1970, AJ, 75, 507
Hartkopf, W. I., & McAlister, H. A. 1984, PASP, 96, 105 (HAR84)
Hartkopf, W. I., McAlister, H. A., & Franz, O. G. 1989, AJ, 98, 1014
Hartkopf, W. I., McAlister, H. A., Mason, B. D., Barry, D. J., Turner, N. H. & Fu, H.-H. 1994, AJ, 108, 2299 (HAR94)
Hoffleit, D., & Jaschek, C. 1982, The Bright Star Catalogue, 4th Ed. (Yale University Observatory, New Haven)
Ianna, P. A. 1979, AJ, 84, 127
Ianna, P. A., McNamara, B. R., & Greason, M. R. 1990, AJ, 99, 415
Ismailov, R. M. 1992, A&AS, 96, 373 (ISM92)
Johnson, H. L. 1966, ARA&A, 4, 193
Keenan, P. C., & McNeil, R. C. 1989, ApJS, 71, 245
Mason, B. D. 1994, Ph.D. dissertation, Georgia State University
McAlister, H. A. 1978, ApJ, 225, 932 (McA78)
McAlister, H. A., Hartkopf, W. I., Hendry, E., Gaston, B. J., M., & Fekel, F. C. 1984, ApJS, 54, 251 (McA84)
McAlister, H. A., Hartkopf, W. I., Hutter, D. J., Shara, M. M., & Franz, O. G. 1987, AJ, 93, 183 (McA87)
McAlister, H. A., & Hendry, E. M. 1981, PASP, 93, 221 (McA81)
McAlister, H. A., & Ianna, P. A. 1974, PASP, 86, 769
Morgan, W. W., Harris, D. L., & Johnson, H. L. 1953, ApJ, 118, 92
Morgan, W. W., & Keenan, P. C. 1973, ARA&A, 12, 29
Neckel, H. 1986, A&A, 169, 194
Olsen, E. H. 1984, A&AS, 57, 443
Pallavicini, R., Cerruti-Sola, M., & Duncan, D. K. 1987, A&A, 174, 116
Parsons, S. B., & Montemayor, T. J. 1982, ApJS, 49, 175
Popper, D. M. 1993, ApJ, 404, L67
Popper, D. M., Lacy, C. H., Frueh, M. L., & Turner, A. E. 1986, AJ, 91, 383
Scarfe, C. D., Batten, A. H., & Fletcher, J. M. 1990, Publ. Dom. Astrophys. Obs., 18, 21
Soderblom, D. R., Jones, B. F., Balachandran, S., Staufer, J. R., Duncan, D. K., Fedele, S. B., & Hudon, J. D. 1993, AJ, 106, 1059
Soderblom, D. R., & Mayor, M. 1993, AJ, 105, 226
Sowell, J. R., & Wilson, J. W. 1993, PASP, 105, 36
Stockton, R. A., & Fekel, F. C. 1992, MNRAS, 256, 575
Strassmeier, K. G., & Fekel, F. C. 1990, A&A, 230, 389
Tokovinin, A. A. 1987, AZh, 64, 196 (SvA, 31, 98)
Tokovinin, A. A. 1992, in Complementary Approaches to Double and Multiple Star Research, IAU Colloquium No. 135, ASP Conf. Ser., Vol. 32, edited by H. A. McAlister and W. I. Hartkopf (ASP, San Francisco), p. 573
van Altena, W. F. 1974, AJ, 79, 831
van de Kamp, P. 1967, Principles of Astrometry (Freeman, San Francisco), p. 167
Woolley, R., Epps, E. A., Penston, M. J., & Pocock, S. 1970, R. Obs. Ann. (Royal Greenwich Observatory, Herstmonceux), No. 5
Young, R. K. 1945, Publ. David Dunlap Obs., 1, 309